

First principles study of electronic and structural properties of CuO

Burak Himmetoglu, Renata M. Wentzcovitch and Matteo Cococcioni

Department of Chemical Engineering and Materials Science,

University of Minnesota, Minneapolis, Minnesota 55455

(Dated: November 27, 2024)

We investigate the electronic and structural properties of CuO, which shows significant deviations from the trends obeyed by other transition-metal monoxides. Using an extended Hubbard corrective functional, we uncover an orbitally ordered insulating ground state for the cubic phase of this material, which was expected but never found before. This insulating state results from a fine balance between the tendency of Cu to complete its d-shell and Hund's rule magnetism. Starting from the ground state for the cubic phase, we also study tetragonal distortions of the unit cell (recently reported in experiments), the consequent electronic reorganizations and identify the equilibrium structure. Our calculations reveal an unexpected richness of possible magnetic and orbital orders, relatively close in energy to the ground state, whose stability depends on the sign and entity of distortion.

I. INTRODUCTION

Among the transition-metal oxide (TMO) compounds, CuO shows quite peculiar characteristics. At variance with other TMOs, which crystallize in a cubic rock-salt structure (with possible rhombohedral distortions), it is found to have a lower-symmetry monoclinic cell¹⁻³. Similarly to other TMOs, CuO has an antiferromagnetic ground state¹. However, its Néel temperature ($T_N \simeq 220K$) is substantially lower than the (expected) linear trend followed by other TMOs (The Néel temperatures of TMOs are observed to increase almost linearly, from MnO ($T_N \simeq 116K$) to NiO ($T_N \simeq 525K$), with the nuclear charge of the transition metal). The reduction in T_N seems to be related to the fact that the monoclinic ground state is stabilized by a Jahn-Teller structural distortion, which yields lower effective exchange interaction compared to a cubic structure⁴.

In spite of the fact that it is not stable, studying the cubic phase of this material is still interesting as a reference point for the characterization of all the electronic mechanisms correlating to the structural deformations. In addition, cubic CuO has also been recently considered as a proxy structure for high T_c superconducting cuprates⁵, to investigate the interplay between “d” and “p” electrons. Although cubic CuO has never been observed experimentally, a tetragonal phase of CuO (i.e. elongated rock-salt cell along one crystal axis) has recently been deposited on substrates of SrTiO₃ thin films⁶. The tetragonal phase of CuO has become a subject of several theoretical studies based on density functional theory (DFT)^{5,7,8}. All the DFT studies have predicted, in agreement with the experimental results, a distortion characterized by $1.1 \lesssim c/a \lesssim 1.3$ ^{5,7,8} (where c denotes the elongated lattice parameter and a denotes the ones in the perpendicular direction). Among possible magnetic configurations, the antiferromagnetic-II (AF-II), characterized by ferromagnetic (111) planes with opposite spins with respect to their neighbors, and the AF-IV, characterized by ferromagnetic (110) planes with opposite spins with respect to their neighbors, configurations compete

for minimum energy. Self-interaction corrected density functional (SIC) based study predicts an AF-II ordered ground state with $c/a \simeq 1.1$ ⁷, while the hybrid density functionals predict an AF-IV ordered ground state with $c/a \simeq 1.3$ ⁸. In both studies, a local energy minimum was also identified at $c/a \simeq 0.9$. At this local minimum, the magnetic structure was found to be AF-II. DFT+U, limited only to the AF-II magnetic ordering, yields an equilibrium structure with $c/a \simeq 1.1$ ⁵. In all these studies, the cubic phase (i.e. the limit when $c/a = 1$) is found to be metallic and corresponding to a local peak in the energy. However, as pointed out in other studies⁵, it seems quite unlikely that the insulating structures with $c/a < 1$ and $c/a > 1$ are “connected” by a metallic state at $c/a = 1$. Instead, an insulating state for the cubic structure seems more reasonable.

In this paper, we revisit the cubic and tetragonal phases of CuO to investigate the underlying mechanism characterizing the electronic, magnetic and structural properties of this compound using a DFT+U based corrective functional within the AF-II magnetic order. We find an insulating ground state for the cubic phase of CuO, that was expected but never found before in the literature. Starting from this insulating ground state for the cubic cell, we also study tetragonal distortions and find an equilibrium structure in agreement with experiments and previous calculations. The properties of this ground state are controlled by an interesting interplay between Hund's rule magnetism and electronic localization. We believe that similar effects could also play an important role in more complex cuprate materials.

The paper is organized as follows: in section II we summarize the DFT+U method we have used. In section III we discuss the electronic structure of the cubic phase, from DFT and DFT+U functionals. In section IV, we introduce an extension of the DFT+U method to include an effective exchange parameter J (DFT+U+ J) and discuss the resulting electronic structure of the cubic phase. In section V we study elongated structures and compare our results with those from the existing literature. Finally, in section VI we summarize our findings and pro-

pose some conclusions.

II. DFT+U METHOD

In this study, we employ the Hubbard model DFT+U corrective scheme, originally introduced in ⁹⁻¹¹, that has become one of the most popular choices to study systems characterized by strong electronic correlations. Although not able to capture all the possible correlated ground states, this corrective scheme has proved to be quite versatile in the description of the ground states of several transition metal compounds^{12,13}, minerals of the Earth's interior¹²⁻¹⁷, molecular complexes¹⁸⁻²¹, TMOs^{9,10,22-24} and magnetic impurities²⁵. Other more elaborate corrective schemes have also been successfully used in the literature, including self-interaction corrected density functionals²⁶, hybrid density functionals²⁷, dynamical mean field theory²⁸ and reduced density matrix functional theory²⁹. Among these, DFT+U has the advantage to present low computational costs³⁰ and to allow for the efficient calculation of energy derivatives (e.g. forces, stresses, elastic constants etc.). The scheme is based on the addition of a corrective term, inspired from the Hubbard model, that favors Mott localization of electrons on atomic sites. The total energy functional of DFT+U can be written as²²

$$E_{\text{DFT+U}} = E_{\text{DFT}}[n(\mathbf{r})] + E_U[\{n_{m\sigma}^{I\sigma}\}] \quad (1)$$

where E_{DFT} is a standard approximate DFT functional and the Hubbard correction E_U , according to the simplified functional by Dudarev et. al.³¹, is given by

$$E_U = \sum_{I,\sigma} \frac{U^I}{2} \text{Tr}[\mathbf{n}^{I\sigma}(\mathbf{1} - \mathbf{n}^{I\sigma})]. \quad (2)$$

In the above equation, U^I is the Coulomb repulsion parameter on atomic site I (usually applied on the d states of a transition metal) and the occupation matrices \mathbf{n}^I are computed as

$$n_{m\sigma}^{I\sigma} = \sum_{\mathbf{k}v} f_{\mathbf{k}v}^{\sigma} \langle \psi_{\mathbf{k}v}^{\sigma} | \phi_m^I \rangle \langle \phi_{m'}^I | \psi_{\mathbf{k}v}^{\sigma} \rangle \quad (3)$$

where $\psi_{\mathbf{k}v}^{\sigma}$ denote the Kohn-Sham states, $f_{\mathbf{k}v}^{\sigma}$ represent their occupations according to the Fermi-Dirac distribution of their energy, and ϕ_m^I are the atomic orbitals with state index m and centered on site I (In this work we use orthogonalized atomic orbitals, i.e. $\langle \phi_m^I | \phi_{m'}^I \rangle = \delta^{IJ}$, so that orbitals centered on different atomic sites are orthogonal). The representation of occupation matrices in terms of atomic orbitals given in equation (3) is not the only possible choice. The same scheme can be used with different sets of wavefunctions such as Wannier functions^{32,33}, that may offer a more flexible representation of electronic localization. For the same purpose, a recent work introduced an extension to the functional of

equation (2) to include inter-site terms³⁴. While we expect that the inclusion of these terms (especially those between O and Cu) might be important to refine structural properties and to resolve some fine details in the electronic structure, in this paper we neglect them and focus on the atomic (on-site) ones.

In our work, the on-site Coulomb repulsion parameters U^I s are determined using the linear response approach introduced in²². In this work, we have generalized this approach to include the responses of the s states of Cu and O treated as a ‘‘reservoir’’ of charge (instead of the neutralizing ‘‘background’’ of reference²²). Our results show that inter-site interactions (V) are significantly smaller than on site ones (U) and our approximation is justified.

In many cases, the DFT ground state for TMOs have different properties than the DFT+U ground state. For instance, DFT+U could stabilize a magnetic ground state with an insulating gap, while DFT results in a metallic one. Therefore, a more accurate determination of the U^I s should involve a self-consistent procedure, where the linear response computation is repeatedly performed on the DFT+U ground state, until a convergence in their values is reached^{18,34}. This self-consistent procedure proved to be necessary in our study due to the qualitative differences between the DFT and the DFT+U ground states.

In our calculations, we have used the Perdew-Burke-Ernzherof(PBE)³⁵ GGA functional to model the exchange-correlation energy. The Cu and O atoms are represented by ultrasoft pseudopotentials and the kinetic energy and charge density cut-offs are chosen to be 35 Ry and 280 Ry respectively. The Brillouin zone integrations are performed using $8 \times 8 \times 8$ Monkhorst and Pack special point grids³⁶ and a Methfessel and Paxton smearing of the Fermi-Dirac distribution³⁷, with a smearing width of 0.01 Ry. All calculations were performed by using the plane waves pseudopotential ‘pwsf’ code contained in the *Quantum ESPRESSO* package³⁸, where we have implemented the ‘+J’ corrections (as discussed in section IV) starting from the existing DFT+U functional.

III. DFT AND DFT+U CALCULATIONS IN THE CUBIC PHASE

Previous studies of the cubic phase of CuO, based on GGA functionals, predicted a metallic and a non-magnetic ground state. While other TMOs are also predicted to be metallic within GGA, they have an antiferromagnetic ground state with ferromagnetic (111) planes of transition-metal ions alternating with opposite magnetization (AF-II). This magnetic order imposes a rhombohedral symmetry to the cell that sometimes produces a distortion. In this work, CuO is also described with a rhombohedral cell. The unit cell consists of 4 atoms, of which the two Cu atoms have opposite spins. We find that the optimized structure has a lattice parameter of 4.256 Å, which we have adopted for the rest of the

calculations. The density of states obtained with GGA is shown in Fig. 1. As it can be observed, the GGA functional yields a non-magnetic (due to the degeneracy between the two spin states) and metallic ground state with a finite contribution to density of states at the Fermi level. This result could be understood in a simple way by inspecting the splitting of d levels of Cu in a cubic crystal field, schematically represented in Fig. 2. On each Cu^{+2} ion, there are 9 electrons placed in the 3d levels. The d levels are split in the cubic crystal field into a doubly degenerate e_g (higher energy) and triply degenerate t_{2g} states (lower energy). As illustrated in Fig. 2, the metallic character and the non-magnetic ground state are due to the degeneracy of the highest energy e_g states with either spin. On these 4 orbitals, Cu hosts 3 electrons, thus leading to partially filled bands that results in metallic ground state. It is important to notice that O also provides a finite contribution to the density of states at the Fermi level, thus p states (non-magnetic) are also partially filled. This scenario is similar to that of paramagnetic insulators, with the additional complication of spin degeneracy. The orbital degeneracy contributing to

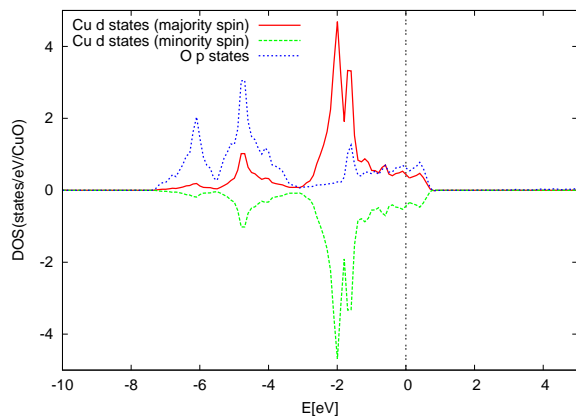


FIG. 1: (Color online) The projected density of states calculated by the GGA functional for cubic CuO.

the metallic character of this ground state is obviously a consequence of the cubic symmetry that makes the e_g states equivalent. This degeneracy cannot be broken by the straight use of DFT+U and since the Hubbard corrective functional is spin diagonal. The density of states of

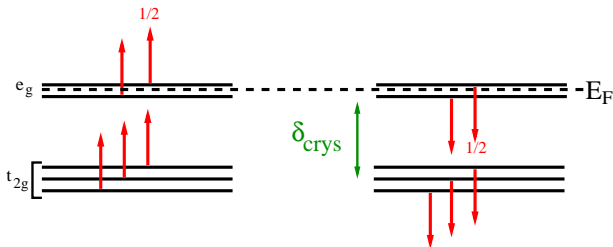


FIG. 2: (Color online) Splitting of d levels in a cubic crystal field.

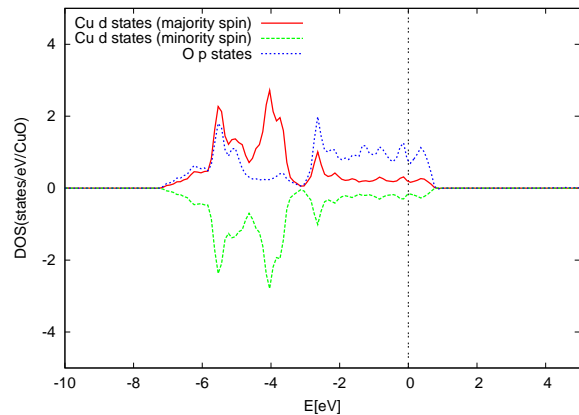


FIG. 3: (Color online) The projected density of states calculated by the $GGA + U$ functional. The on-site Hubbard parameter is $U = 9.79$ eV, which is calculated by the linear response approach²².

the ground state resulting from the $GGA+U$ functional is shown in Fig. 3 where it is evident that the main effect of the Hubbard correction consists in the (probably exaggerated) stabilization of filled d states that shift to lower energies. Both d states (e_g) and p states are left at the Fermi energy. Owing to the presence of O p states around the Fermi level, one might be tempted to extend the Hubbard correction to these states. This was indeed explored in reference³⁹. Fig. 4 shows the density of states

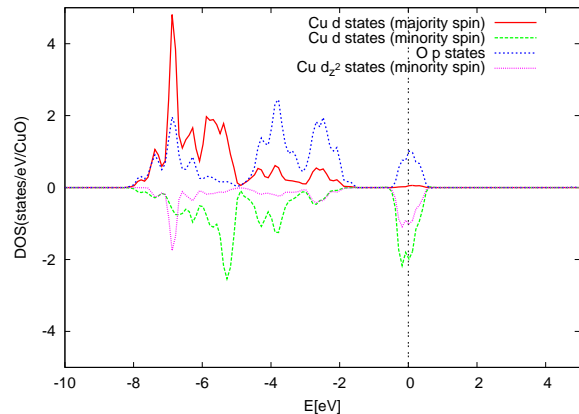


FIG. 4: (Color online) The projected density of states calculated by the $GGA + U + U_p$ functional. The on-site Hubbard parameters are $U = 9.79$ eV and $U_p = 8.47$ eV, which are determined by linear response approach²².

of CuO obtained with a Hubbard correction extended to O p states. The Hubbard U on O p states (U_p) was evaluated using the same linear response method of reference²², that yielded a value of $U_p \simeq 8.47$ eV (vs 9.79 eV of Cu). As evident from the density of states, while the metallic character is preserved, a magnetic ground state now emerges from the lifting of the spin degeneracy. This new situation is schematically illustrated in Fig. 5, where an exchange splitting between opposite spin levels has

resulted in a magnetic ground state. With GGA+U, the non-magnetic ground state leads to an effective cubic symmetry (in spite of the use of the rhombohedral unit cell), therefore the lower energy t_{2g} states are degenerate. The rhombohedral symmetry, induced by the antiferromagnetic order, lifts this degeneracy and splits them into a non-degenerate state with A_{1g} symmetry and a doublet of e_g symmetry as illustrated in Fig. 5. However, the material is still metallic due to the degeneracy of minority spin e_g states. It is important to notice that O p states still contribute to the metallic character (thus resulting in a partially filled p band) with equal contributions from the two spins, in spite of the polarization of the d states. The magnetic ground state in $GGA + U + U_p$ is not directly due to U_p but, rather a consequence of the redistribution of electrons. It is instructive to com-

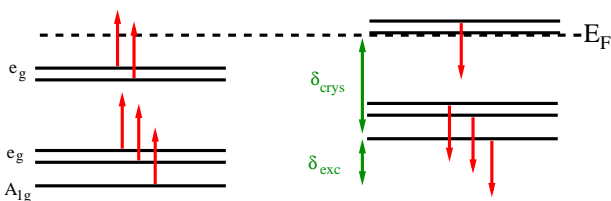


FIG. 5: (Color online) Splitting of Cu d states in a rhombohedral field with the onset of magnetic ordering.

pare at this point, the occupations of d and p orbitals (i.e. traces of $n_{m\sigma}^{I\sigma}$, i given in equation (3)) between the two cases (with $GGA + U$ and $GGA + U + U_p$). For $GGA + U$, we obtain $n_{Cu}^\uparrow(e_g) = n_{Cu}^\downarrow(e_g) \simeq 1.84$, while $n_{O_p} \simeq 4.94$. In the case of $GGA + U + U_p$ we obtain $n_{Cu}^\uparrow(e_g) \simeq 1.96$, $n_{Cu}^\downarrow(e_g) \simeq 1.40$, while $n_{O_p} \simeq 5.27$. The main consequence of using U_p consists in the increase of n_{O_p} and the consequent depression of the population of the d orbitals. Thus, the magnetic ground state seems to be promoted by the partial (and numerically marginal) decrease in the population of d-orbitals. This picture is corroborated by Fig. 4, which shows the explicit contribution to the density of states from d_{z^2} (one of the e_g) states, that accounts for half of the density around the Fermi level. It is also important to notice how the peak in the d_{z^2} density of states correlate with those of the p states, suggesting partial hybridization between Cu and O.

The emergence of the magnetic, albeit metallic ground state is due to the rhombohedral symmetry and cannot be broken by the Hubbard corrections. Thus, the metallic character is a consequence of the crystal symmetry, similar to the case of FeO²². The effective equivalence between the e_g states dictated by the cubic or rhombohedral symmetry could be understood as effectively recovered by the superposition of two (or more) equivalent ground states (of lower symmetry) having either of the e_g orbitals occupied. To check this hypothesis and to obtain one of these states, we have set the calculation in a larger unit cell of lower symmetry. This

unit cell is described by the lattice vectors given by $\mathbf{v}_1 = (-0.5, 0.5, 0)$, $\mathbf{v}_2 = (0, 1, -1)$, $\mathbf{v}_3 = (0.5, 0.5, 1)$ and contains 4 Cu and 4 O atoms. Each magnetic (111) plane contains two Cu atoms in this unit cell and they are treated as of different kinds, albeit associated to the same pseudopotential. This artifact removes the effective equivalence of e_g states even for the 8 atoms cell description of the cubic structure. A similar trick was also used for FeO to stabilize a broken symmetry (orbitally ordered) phase that reproduced the structural distortions of the material under pressure²². The ground state obtained in the 8 atoms cell has slightly lower energy per Cu-O pair ($\Delta E \simeq 1.88 \text{ eV/CuO}$) compared to the rhombohedral 4 atoms unit cell, and thus the broken symmetry configuration is energetically favored.

It is important to remark that even in the broken symmetry phase, an energy gap appears only if a finite Hubbard correction U_p is used on the O p states. Without a Hubbard correction on O p states, the material is predicted to be non-magnetic and a metallic ground state still emerges from the degeneracy of the e_g orbitals with opposite spin. This correction stabilizes the O p states and increases their occupancy at the expense of lowering Cu d state occupancies. Thus, Cu d-orbitals are left with 9 electrons. Hund's rule magnetism favors the localization of the hole in this shell on one of the minority spin e_g states. The calculated d and p occupations reflect the localization of the hole: $n_{Cu}^\uparrow(e_g) \simeq 2.0$, $n_{Cu}^\downarrow(d_{z^2}) \simeq 0.0$, $n_{Cu}^\downarrow(d_{x^2-y^2}) \simeq 1.0$, while $n_{O_p} = 5.51$. These occupations also show that the Cu atoms acquire a finite magnetization which results in an AF-II ground state. The density of states of this ground state is shown in Fig. 6.

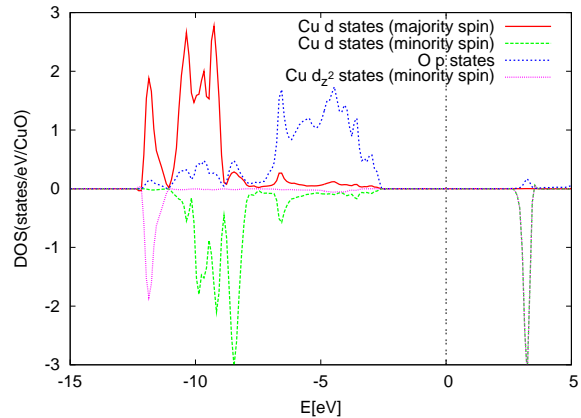


FIG. 6: (Color online) The projected density of states in the broken symmetry phase. The on-site repulsion terms are $U_d = 9.79 \text{ eV}$ and $U_p = 8.47 \text{ eV}$ (calculated from the response of GGA ground state).

Although the application of a Hubbard correction U_p on non-correlated O p states is questionable, this computational experiment is an indication of the fact that this system is characterized by a competition between two opposite tendencies: full occupation of Cu d states and the

stabilization of a magnetic ground state through Hund's rule coupling. If the number of electrons on d states is lower than a certain threshold value, then the Hund's rule magnetism is dominant, otherwise a non-magnetic ground state will appear. This competition is due to two factors: a number of d electrons between 9 and 10 and O p states close in energy to the d states which are able to act as charge "reservoirs" for them. In the next section we further test this hypothesis by an extension to the +U corrective functional that explicitly includes a magnetic coupling J to encourage a magnetic ground state on each Cu atom.

IV. DFT+U+J FUNCTIONAL AND ITS APPLICATION TO THE CUBIC PHASE

The DFT+U functional introduced in equation (2) contains only a minimal set of on-site interaction parameters. In this section, we propose an extension of the DFT+U functional, that includes magnetic (exchange) interactions (DFT+U+J). While this is not new in literature (a review of previous approaches is given in reference⁴⁰), the functional we propose here deviates from previous formulations. The new corrective scheme can be obtained from a general second quantized expression for electron-electron interactions (derived in equation (6) of reference³⁴) given by

$$\hat{V}_{\text{int}} = \frac{1}{2} \sum_{I, J, K, L} \sum_{i, j, k, l} \sum_{\sigma, \sigma'} \langle \phi_i^I \phi_j^J | V_{ee} | \phi_k^K \phi_l^L \rangle \times \hat{c}_{I i \sigma}^\dagger \hat{c}_{J j \sigma'}^\dagger \hat{c}_{K k \sigma'} \hat{c}_{L l \sigma} \quad (4)$$

where capital letters $\{I, \dots K\}$ represent site indices, lowercase letters $\{i, \dots k\}$ represent state indices, $\{\sigma, \sigma'\}$ are spin indices; V_{ee} denote the (screened) Coulomb interaction kernel between electrons and ϕ_i^I denote the atomic wavefunction corresponding to state i centered on site I . The operators $\hat{c}_{I i \sigma}^\dagger, \hat{c}_{I i \sigma}$ create/annihilate electrons with atomic wavefunction ϕ_i^I and spin σ . Assuming that on-site interactions are dominant (especially for the localized d states of transition-metal ions) we keep only terms with $I = J = K = L$ in the above sum. Moreover, we approximate the on-site effective interactions by the atomic averages of Coulomb and exchange terms: $U^I = \frac{1}{(2l+1)^2} \sum_{i,j} \langle \phi_i^I \phi_j^I | V_{ee} | \phi_j^I \phi_i^I \rangle$ and $J^I = \frac{1}{(2l+1)^2} \sum_{i,j} \langle \phi_i^I \phi_j^I | V_{ee} | \phi_i^I \phi_j^I \rangle$. As a result, we obtain:

$$E_{\text{Hub}} = \sum_{I, \sigma} \frac{U^I}{2} \left[(n^{I\sigma})^2 + n^{I\sigma} n^{I-\sigma} - \text{Tr} [\mathbf{n}^{I\sigma} \mathbf{n}^{I\sigma}] \right] + \frac{J^I}{2} \left[\text{Tr} [\mathbf{n}^{I\sigma} \mathbf{n}^{I\sigma} + \mathbf{n}^{I\sigma} \mathbf{n}^{I-\sigma}] - (n^{I\sigma})^2 \right] \quad (5)$$

where the occupations $n_{i_j}^{I\sigma} = \langle \hat{c}_{I i \sigma}^\dagger \hat{c}_{I j \sigma} \rangle$ are computed using the expression given in (3); $n^{I\sigma} = \text{Tr}[\mathbf{n}^{I\sigma}]$ and

$n^I = \sum_{\sigma} n^{I\sigma}$. We introduce a double counting term to be subtracted from E_{Hub} that is evaluated as the mean field approximation of (5) in the fully localized limit⁴¹, where each atomic orbital is either filled by a single electron or totally empty. In this approximation we have:

$$\text{Tr}[\mathbf{n}^{I\sigma} \mathbf{n}^{I\sigma}] \rightarrow n^{I\sigma}, \quad \text{Tr}[\mathbf{n}^{I\sigma} \mathbf{n}^{I-\sigma}] \rightarrow n^{I\sigma_{\text{min}}}$$

where σ_{min} denotes the minority spin. The above expression is true for both magnetic and non-magnetic systems (for non-magnetic systems $\sigma_{\text{min}} = \sigma$, since spin up and down densities are equivalent). In the fully localized limit, the entire double counting term thus reads

$$E_{\text{dc}} = \sum_I \frac{U^I}{2} n^I (n^I - 1) - \sum_{I, \sigma} \frac{J^I}{2} n^{I\sigma} (n^{I\sigma} - 1) + \sum_I J^I n^{I\sigma_{\text{min}}}. \quad (6)$$

The first term in the above equation is already included in the standard DFT+U functional given in equation (2). After some algebra, we easily obtain the expression of the corrective functional as

$$E_{\text{Hub}} - E_{\text{dc}} = \sum_{I, \sigma} \frac{U^I - J^I}{2} \text{Tr}[\mathbf{n}^{I\sigma} (\mathbf{1} - \mathbf{n}^{I\sigma})] + \sum_{I, \sigma} \frac{J^I}{2} \{ \text{Tr}[\mathbf{n}^{I\sigma} \mathbf{n}^{I-\sigma}] - 2 \delta^{\sigma \sigma_{\text{min}}} n^{I\sigma} \}. \quad (7)$$

Comparing (2) and (7), one can see that the on-site Coulomb repulsion parameter (U^I) is effectively reduced by J^I for interactions between electrons of parallel spin and a positive J term further discourages anti-aligned spins on the same site. As a result, the functional given in equation (7) encourages magnetic ordering. Within the simple Dudarev model³¹, the inclusion of J has only been considered as the effective renormalization of U (i.e. $U^I \rightarrow U^I - J^I$) and the terms in the second line of (7) were not included. The quadratic term in the second line of equation (7) can be explicitated as

$$\sum_{I, \sigma} \frac{J^I}{2} n_{m m'}^{I\sigma} n_{m' m}^{I-\sigma}. \quad (8)$$

Since the occupations can be understood as the expectation value $n_{m, m'}^{I\sigma} = \langle \hat{c}_{I m \sigma}^\dagger \hat{c}_{I m' \sigma} \rangle$, this term describes an "orbital exchange" between electrons of opposite spins (e.g. up spin electron from m' to m and down spin electron from m to m'). It is important to notice that this term is genuinely beyond Hartree-Fock. In fact, a single Slater determinant containing the four states $m \uparrow, m \downarrow, m' \uparrow, m' \downarrow$ would produce no interaction term like the one above. So this contribution to the corrective functional can be understood as resulting from the interactions between configurations that differ from each other by two single electron states. In this context, the

use of occupation numbers computed as in equation (3) is not legitimate (these configurations do not contribute together to any single term of the electronic charge density). Thus the expression of the J term given in equation (7), based on a product of $\mathbf{n}^{I\sigma}$ and $\mathbf{n}^{I-\sigma}$ is an approximation of a functional that would require the calculation of the 2-body density matrix. Based on this reasoning, we argue that these interaction terms are not captured by approximate DFT functionals, where the total energy is a functional of the one-body electron density. Therefore, we can suppose that they are completely missing from the DFT functional and we can neglect them in the double counting term that thus leads to

$$E_{\text{dc}} = E_{\text{dc}}^U - \sum_{I,\sigma} \frac{J^I}{2} n^{I\sigma} (n^{I\sigma} - 1) \quad (9)$$

where $E_{\text{dc}}^U = 1/2 \sum_I U^I n^I (n^I - 1)$. The double counting term (9) was previously considered in^{42,43}. It corresponds to the sum over like-spin electron pairs multiplied by the exchange parameter, and takes into account the total exchange energy in an average way. As a matter of fact, we have verified that both dc terms (6) and (9) yield the same ground state for CuO. However, the one in equation (9) is numerically more stable and we have adopted it in all calculations presented here.

Although never included in corrective DFT-based functionals, terms like in equation (8) were introduced in numerical studies based on model Hamiltonians^{44,45}.

In order to calculate the Hubbard exchange parameter J , we have extended the linear response approach²² used in the previous section and we have computed the responses of on-site magnetizations $m^J = n^{J\uparrow} - n^{J\downarrow}$ to a magnetic perturbation βm^I . Modeling the total energy of the solid with the double counting term (either equation (6) or (9)), and rewriting it in terms of the on-site occupations n^I and magnetizations m^I , we can calculate the exchange parameter J^I from $\partial^2 E / (\partial m^I)^2 = -J^I / 2$. The second derivative of the energy with respect to on-site magnetizations are calculated using the response matrices $\chi_{IJ} = \partial m^I / \partial \beta^J$ so that $J^I = -2[(\chi^0)_{II}^{-1} - (\chi)_{II}^{-1}]$. In this equation χ^0 denotes the bare response matrix which is computed from the non-interacting Kohn-Sham problem, which needs to be subtracted from the response of the interacting system to obtain the value of J^I as described in²².

In this work, the J parameter was computed using 32 atoms supercell and we found that $J \simeq 2.5 \text{ eV}$ (The 16 atoms supercell employed for the calculation of U proved to be insufficient for obtaining linearly behaving magnetic response matrices). We would like to stress that the values $U \simeq 9.79 \text{ eV}$ used in the previous section and $J \simeq 2.5 \text{ eV}$ are obtained by the response of the GGA ground state, and are used as “test” values in the previous and current sections. More precise values are obtained by a self-consistent procedure (i.e. by recomputing the responses using the $GGA + U$ ground state) for the discussion of elongated structures in the next section.

In agreement with the discussion at the end of the previous section, the explicit account of magnetic interactions through the new functional results in an insulating and antiferromagnetic ground state (with a broken symmetry phase). The resulting density of states is shown in Fig. 7. The exchange interaction parameter J enhances the splitting between opposite spin electrons and favors a magnetic (insulating) state. As can be seen in Fig. 7, the

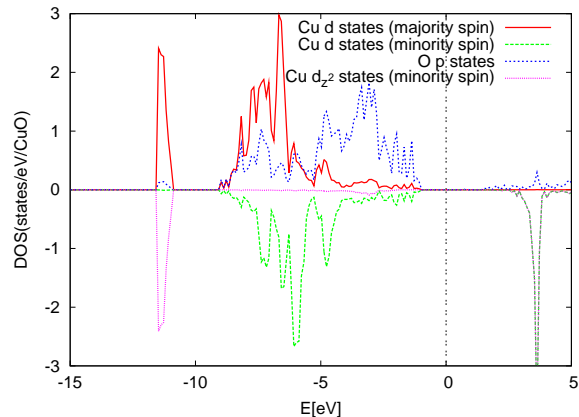


FIG. 7: (Color online) The projected density of states in the broken symmetry phase. The Hubbard parameters for the Cu-d states are $U = 9.79 \text{ eV}$ and $J = 2.50 \text{ eV}$ (calculated from the response of GGA ground state).

$GGA+U+J$ functional localizes a hole in the d_{z^2} state on each Cu atom, as for the case of the $GGA+U+U_p$ ground state, while all other d states are filled and lie below the gap. This result suggests that the insulating ground state is stabilized by magnetic interactions. Recently, the importance of the exchange coupling J in favoring metallic or insulating ground states of correlated systems has also been verified using the dynamical mean field theory⁴⁶. However, magnetic and non-magnetic ground states are very close in energy. We hypothesize that this balance could be inverted by doping. We have also checked that it is possible to localize the hole on the $d_{x^2-y^2}$ orbital or a configuration with mixed occupations (i.e. one hole localized on $d_{x^2-y^2}$ on one Cu atom and one hole localized on d_{z^2} on the other Cu atom of the same (111) plane). These configurations have slightly higher energies than the ground state we have discussed above (the state with mixed occupations is about 0.3 eV/cell higher in energy than the ground state, and the configuration with the $d_{x^2-y^2}$ hole is about 0.5 eV/cell higher in energy than the ground state). The relatively low energy difference between them is due to the cubic crystal structure which is broken/lifted on e_g states for the electrons.

As pointed out in the introduction, the broken symmetry insulating state in the cubic phase was never found before, and the degeneracy between the e_g levels was lifted through a tetragonal distortion in other works^{5,7,8}. We have shown instead, that the symmetry can be broken even for the cubic cell (with a lower symmetry 8 atoms

unit cell, effectively corresponding to the cubic structure) and that an insulating state can result from magnetic interactions. In the next section, we study elongated structures and determine their ground state properties using the 8 atoms cell.

V. TETRAGONALLY DISTORTED STRUCTURES

In this section we discuss the ground state properties of the tetragonally distorted structures. We limit our study only to the case of AF-II ordering (unlike some previous studies^{7,8}, which also considered other magnetic configurations) and determine the value of the tetragonal distortion c/a corresponding to lowest energy. To do so, we have calculated the Hubbard parameter U at each value of c/a between 0.9 and 1.2 using the linear response approach in a self-consistent procedure, while the J parameter was fixed to the value obtained from the cubic cell and just with the GGA response (we assumed its variation to be less important). In fact, the value of the parameter J must be calculated from the response of a non-magnetic ground state (i.e. the GGA ground state of cubic phase of CuO), since the linearity of the response matrices is not preserved when the ground state is magnetic (i.e. GGA+U+J ground state, or any tetragonally distorted phase). Therefore, we have limited the calculation of J to the non-magnetic phase. The U parameters on the other hand, are computed self-consistently until their value converges within an accuracy of about $0.2 eV$. The value of the lattice parameter a was fixed, so the volume of the cell varies between different calculations. However, we have also studied a deformation at fixed volume and obtained very similar results, which will not be discussed in this work. In Fig. 8 we show the calculated values of Hubbard U parameter as a function of c/a . We show both the values calculated from GGA response (the green line) and the values that are calculated self-consistently (the red line). The self-consistent values of the U parameters are smaller than the ones calculated from the GGA response, especially around the region close to $c/a \sim 1$ (i.e. the cubic phase). This difference is due to the fact that the GGA ground state in the cubic structure is metallic and paramagnetic, while the $GGA + U + J$ ground state is insulating and antiferromagnetic. This effect is also visible at large tetragonal distortions, however it is less dramatic than for $c/a \simeq 1$, since GGA yields ground states that are antiferromagnetic for $c/a \gtrsim 1.1$ and $c/a \lesssim 0.9$. From our calculations, we find that the hole in the d states of Cu atoms are localized on the $d_{x^2-y^2}$ orbitals for $c/a > 1$ and on the d_{z^2} orbitals for $c/a \leq 1$. These orbital configurations are expected, since the elongation of the z-axis lowers the Coulomb repulsion energy of electrons localized on d_{z^2} orbitals. Therefore, the localization of the hole in the $d_{x^2-y^2}$ orbitals (or, equivalently, the localization of an electron on the d_{z^2} orbitals) is energetically favor-

able for $c/a > 1$ and vice-versa. The minimum energy configuration was found to be at $c/a \simeq 1.15$ as shown in Fig. 9. The energy differences for different values of c/a are in overall agreement with the findings of previous studies^{5,7}. We have also calculated the energy band gaps

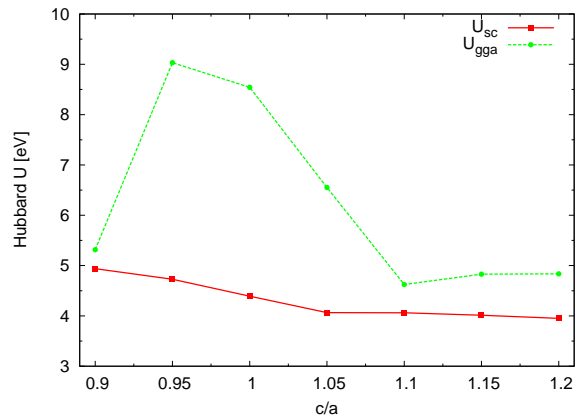


FIG. 8: (Color online) Calculated U_d for each value of c/a . The green line shows the linear response values calculated from the GGA response and the red line shows the self-consistently calculated values.

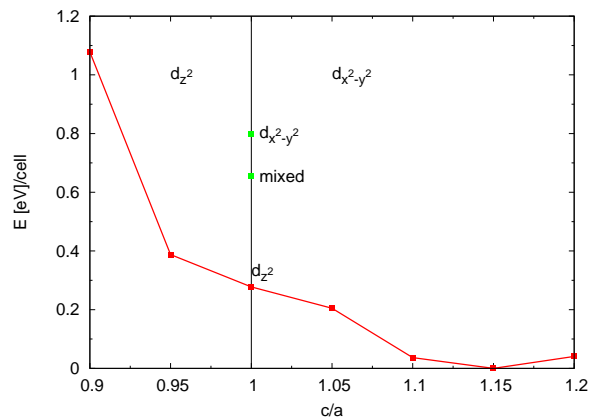


FIG. 9: (Color online) The ground state energy profile as a function of the tetragonal distortion c/a . The orbital localizations of the holes on Cu d states for $c/a > 1$ and for $c/a < 1$ are labeled. The ground state energies of different hole localizations for the cubic phase are also shown.

for each structure, which lie between $1.4 eV$ ($c/a = 0.9$) and $0.4 eV$ ($c/a = 1.2$) and decreases with c/a . The energy band gap for monoclinic CuO was determined to lie between $1.21 eV$ and $1.7 eV$ experimentally^{47,48}. The largest value of $1.4 eV$ we have obtained is within the experimental range, but for larger values of c/a , the gap becomes lower than the experimental one. The difference is probably related with the fact that the structures we are considering have different symmetry than the ones studied experimentally.

The value of the tetragonal distortion we found for the

most stable configuration ($c/a \simeq 1.15$) is lower than the experimentally observed value of $c/a \simeq 1.35$. This difference could be related to the fact that our calculations do not take into account surface effects (strains) which are important for ultrathin films of tetragonal CuO grown on the SrTiO₃ support. Indeed, it was recently shown that when surface effects are taken into account, better agreement with experimental results are obtained⁴⁹. The c/a we found is in agreement with the results of references^{5,7}, however it is lower than $c/a \simeq 1.377$ of reference⁸. This difference could be related with the different localization properties of the hybrid-density functionals used in⁸ and DFT+U. The functional used in this work strongly localizes the electrons on atomic sites, and is less accurate in representing hybridization effects that could be important in CuO. The disagreement could be removed with the use of the inter-site interactions, which was shown to improve structural properties³⁴. In addition, a structurally consistent calculation of the Hubbard parameters as was done in¹³, is expected to result in more precise structural properties. Finally, we would like to stress that the local minimum located at $c/a \simeq 0.95$, which was identified in some previous works^{7,8}, has disappeared in our calculations, as can be seen in Fig. 9. Based on our results, we think that the local minimum was the consequence of the artificially high energy of the metallic cubic phase compared to the distorted ones. We argue that the metallic state obtained with the approximate DFT functional for $c/a = 1$ results from the degeneracy of e_g orbitals which is the result of cubic symmetry.

VI. SUMMARY

In this work we have studied the electronic structure of CuO both in the cubic and tetragonal phases. We have identified the insulating state in the cubic structure, which was expected but never found before. The emer-

gence of the cubic insulating state requires the breaking of symmetry in the electronic structure and leads to an orbitally ordered ground state. We have found that the insulating ground state results from a delicate balance between two tendencies: filling the d shell of Cu with (nearly) 10 electrons and localizing a hole on one of the e_g states to stabilize a magnetic ground state. After stabilizing the magnetic ground states, we have identified several local energy minima in the cubic configuration (paramagnetic, with holes localized on $d_{x^2-y^2}$ orbitals, on d_{z^2} orbitals and with mixed type of localizations) at slightly higher energies. We have also studied tetragonal distortions in the system and found the lowest energy configuration to be at $c/a \simeq 1.15$. Our findings are in reasonable agreement with experimental results, although inclusion of inter-site interactions in the functional could improve the agreement. Finally, we clarified the transition (through the cubic phase with $c/a = 1$) between the two different localization regimes of Cu d electrons (on $d_{x^2-y^2}$ orbitals for $c/a \leq 1$ and on d_{z^2} orbitals for $c/a > 1$) and suggested that the metallic state predicted by approximate DFT functional for the cubic phase is the result of the degeneracy between e_g states, artificially enforced by the symmetry of the crystal. We believe that the interplay between orbital ordering and magnetism and the interaction between the d and p electrons, highlighted in this work, will be of interest in studying high T_c superconductors, where similar electronic dynamics and competitions between charge and spin degrees of freedom are believed to play an important role.

Acknowledgments

We acknowledge support from the NSF grant EAR-0810272, and the Minnesota Supercomputing Institute (MSI) for providing computational resources. We would also like to thank P. W. Grant for proposing the problem.

-
- ¹ T. Kimura, Y. Sekio, H. Nakamura, T. Siegrist, and A. Ramirez, *Nat. Mater.* **7**, 291 (2008).
² B. Yang, T. Thurston, J. Tranquada, and G. Shirane, *Phys. Rev. B* **39**, 4343 (1989).
³ S. Asbrink and L. Norrby, *Acta Crystallogr., Sect. B: Struct. Sci* **26**, 8 (1970).
⁴ A. Filippetti and V. Fiorentini, *Phys. Rev. Lett.* **95**, 86405 (2005).
⁵ P. Grant, in *J. Phys. Conf. Ser.* (IOP Publishing, 2008), vol. 129, p. 012042.
⁶ W. Siemons, G. Koster, D. Blank, R. Hammond, T. Geballe, and M. Beasley, *Phys. Rev. B* **79**, 195122 (2009).
⁷ G. Peralta, D. Puggioni, A. Filippetti, and V. Fiorentini, *Phys. Rev. B* **80**, 140408 (2009).
⁸ X. Chen, C. Fu, C. Franchini, and R. Podloucky, *Phys. Rev. B* **80**, 94527 (2009).
⁹ V. Anisimov, J. Zaanen, and O. Andersen, *Phys. Rev. B*

- 44**, 943 (1991).
¹⁰ V. Anisimov, I. Solovyev, M. Korotin, M. Czyżyk, and G. Sawatzky, *Phys. Rev. B* **48**, 16929 (1993).
¹¹ I. Solovyev, P. Dederichs, and V. Anisimov, *Phys. Rev. B* **50**, 16861 (1994).
¹² H. Hsu, P. Blaha, R. Wentzcovitch, and C. Leighton, *Phys. Rev. B* **82**, 100406 (2010).
¹³ H. Hsu, K. Umemoto, M. Cococcioni, and R. Wentzcovitch, *Phys. Rev. B* **79**, 125124 (2009).
¹⁴ H. Hsu, P. Blaha, M. Cococcioni, and R. Wentzcovitch, *Phys. Rev. Lett.* **106**, 118501 (2011), ISSN 1079-7114.
¹⁵ H. Hsu, K. Umemoto, M. Cococcioni, and R. Wentzcovitch, *Phys. Earth Planet. Inter.* (2010).
¹⁶ S. Stackhouse, L. Stixrude, and B. Karki, *Earth Planet. Sci. Lett.* **289**, 449 (2010).
¹⁷ S. Stackhouse, J. Brodholt, and G. Price, *Earth Planet. Sci. Lett.* **253**, 282 (2007).
¹⁸ H. Kulik, M. Cococcioni, D. Scherlis, and N. Marzari,

- Phys. Rev. Lett. **97**, 103001 (2006).
- ¹⁹ D. Scherlis, M. Cococcioni, P. Sit, and N. Marzari, J. Phys. Chem. B **111**, 7384 (2007).
 - ²⁰ K. Leung, I. Nielsen, N. Sai, C. Medforth, and J. Shelnutt, J. Phys. Chem. A (2010).
 - ²¹ H. Kulik and N. Marzari, J. Chem. Phys. **133**, 114103 (2010).
 - ²² M. Cococcioni and S. De Gironcoli, Phys. Rev. B **71**, 35105 (2005).
 - ²³ I. Mazin and V. Anisimov, Phys. Rev. B **55**, 12822 (1997).
 - ²⁴ I. Solovyev, A. Liechtenstein, and K. Terakura, J. Magn. Magn. Mater. **185**, 118 (1998).
 - ²⁵ G. Mattioli, P. Alippi, F. Filippone, R. Caminiti, and A. Amore Bonapasta, J. Phys. Chem. C **114**, 21694 (2010).
 - ²⁶ A. Filippetti and N. Spaldin, Phys. Rev. B **67**, 125109 (2003).
 - ²⁷ A. Becke, J. Chem. Phys. **98**, 1372 (1993).
 - ²⁸ A. Lichtenstein and M. Katsnelson, Phys. Rev. B **57**, 6884 (1998).
 - ²⁹ S. Sharma, J. Dewhurst, N. Lathiotakis, and E. Gross, Phys. Rev. B **78**, 201103 (2008).
 - ³⁰ W. Setyawan and S. Curtarolo, Comp. Mater. Sci. **49**, 299 (2010).
 - ³¹ S. Dudarev, G. Botton, S. Savrasov, C. Humphreys, and A. Sutton, Phys. Rev. B **57**, 1505 (1998).
 - ³² D. O'Regan, N. Hine, M. Payne, and A. Mostofi, Phys. Rev. B **82**, 081102 (2010).
 - ³³ V. Mazurenko, S. Skornyakov, A. Kozhevnikov, F. Mila, and V. Anisimov, Phys. Rev. B **75**, 224408 (2007).
 - ³⁴ V. Campo Jr and M. Cococcioni, J. Phys. Condens. Matter **22**, 055602 (2010).
 - ³⁵ J. Perdew, K. Burke, and M. Ernzerhof, Phys. Rev. Lett **77**, 3865 (1996).
 - ³⁶ H. Monkhorst and J. Pack, Phys. Rev. B **13**, 5188 (1976).
 - ³⁷ M. Methfessel and A. Paxton, Phys. Rev. B **40**, 3616 (1989).
 - ³⁸ P. Giannozzi, S. Baroni, N. Bonini, M. Calandra, R. Car, C. Cavazzoni, D. Ceresoli, G. Chiarotti, M. Cococcioni, I. Dabo, et al., J. Phys. Condens. Matter **21**, 395502 (2009).
 - ³⁹ I. A. Nekrasov, M. A. Korotin, and V. I. Anisimov, ArXiv (2000), arXiv:cond-mat/0009107.
 - ⁴⁰ E. Ylvisaker, W. Pickett, and K. Koepernik, Phys. Rev. B **79**, 035103 (2009).
 - ⁴¹ A. Petukhov, I. Mazin, L. Chioncel, and A. Lichtenstein, Phys. Rev. B **67**, 153106 (2003).
 - ⁴² V. Anisimov, F. Aryasetiawan, and A. Lichtenstein, J. Phys.: Condens. Matter **9**, 767 (1997).
 - ⁴³ M. Czyżyk and G. Sawatzky, Phys. Rev. B **49**, 14211 (1994).
 - ⁴⁴ J. Yoshitake and Y. Motome, Arxiv preprint arXiv:1105.5757 (2011).
 - ⁴⁵ D. L. H. L. Y.M. Quan, L.J. Zou, Arxiv preprint arXiv:1106.3487 (2011).
 - ⁴⁶ L. Medici, J. Mravlje, and A. Georges, Arxiv preprint arXiv:1106.0815 (2011).
 - ⁴⁷ F. Koffyberg and F. Benko, J. Appl. Phys. **53**, 1173 (1982).
 - ⁴⁸ F. Marabelli, G. Parravicini, and F. Salghetti-Drioli, Phys. Rev. B **52**, 1433 (1995).
 - ⁴⁹ C. Franchini, X. Chen, and R. Podloucky, J. Phys. Condens. Matter **23**, 045004 (2011).

